Analysis of the low-energy electron-recoil spectrum of the CDMS experiment

Z. Ahmed,[1] D. S. Akerib,[2] S. Arrenberg,[17] C. N. Bailey,[2] D. Balakishiyeva,[15] L. Baudis,[17] D. A. Bauer,[3] J. Beaty,[16]
P. L. Brink,[9] T. Bruch,[17] R. Bunker,[13] B. Cabrera,[9] D. O. Caldwell,[13] J. Cooley,[9] P. Cushman,[16] F. DeJongh,[3]
M. R. Dragowsky,[2] L. Duong,[16] E. Figueroa-Feliciano,[5] J. Filippini,[12,1] M. Fritts,[16] S. R. Golwala,[1] D. R. Grant,[2] J. Hall,[3]
R. Hennings-Yeomans,[2] S. Hertel,[5] D. Holmgren,[3] L. Hsu,[3] M. E. Huber,[14] O. Kamaev,[16] M. Kiveni,[10] M. Kos,[10]
S. W. Leman,[5] R. Mahapatra,[11] V. Mandic,[16] D. Moore,[1] K. A. McCarthy,[5] N. Mirabolfathi,[12] H. Nelson,[13]
R. W. Ogburn,[9,1] M. Pyle,[9] X. Qiu,[16] E. Ramberg,[3] W. Rau,[6] A. Reisetter,[7,16] T. Saab,[15] B. Sadoulet,[4,12]
J. Sander,[13] R. W. Schnee,[10] D. N. Seitz,[12] B. Serfass,[12] K. M. Sundqvist,[12] G. Wang,[1] P. Wikus,[5] S. Yellin,[9,13]
J. Yoo,[3] and B. A. Young[8]

(CDMS Collaboration)

[1]*Department of Physics, California Institute of Technology, Pasadena, California 91125, USA*
[2]*Department of Physics, Case Western Reserve University, Cleveland, Ohio 44106, USA*
[3]*Fermi National Accelerator Laboratory, Batavia, Illinois 60510, USA*
[4]*Lawrence Berkeley National Laboratory, Berkeley, California 94720, USA*
[5]*Department of Physics, Massachusetts Institute of Technology, Cambridge, Massachusetts 02139, USA*
[6]*Department of Physics, Queen's University, Kingston, ON, Canada, K7L 3N6*
[7]*Department of Physics, Saint Olaf College, Northfield, Minnesota 55057, USA*
[8]*Department of Physics, Santa Clara University, Santa Clara, California 95053, USA*
[9]*Department of Physics, Stanford University, Stanford, California 94305, USA*
[10]*Department of Physics, Syracuse University, Syracuse, New York 13244, USA*
[11]*Department of Physics, Texas A&M University, College Station, Texas 93106, USA*
[12]*Department of Physics, University of California, Berkeley, California 94720, USA*
[13]*Department of Physics, University of California, Santa Barbara, California 93106, USA*
[14]*Departments of Phys. & Elec. Engr., University of Colorado Denver, Denver, Colorado 80217, USA*
[15]*Department of Physics, University of Florida, Gainesville, Florida 32611, USA*
[16]*School of Physics & Astronomy, University of Minnesota, Minneapolis, Minnesota 55455, USA*
[17]*Physics Institute, University of Zürich, Zürich, Switzerland*

We report on the analysis of the low-energy electron-recoil spectrum from the CDMS II experiment using data with an exposure of 443.2 kg-days. The analysis provides details on the observed counting rate and possible background sources in the energy range of 2–8.5 keV. We find no significant excess of a peaked contribution to the total counting rate above the background model, and compare this observation to the recent DAMA results. In the framework of a conversion of a dark matter particle into electromagnetic energy, our 90% confidence level upper limit of 0.246 events/kg/day at 3.15 keV is lower than the total rate above background observed by DAMA. In absence of any specific particle physics model to provide the scaling in cross section between NaI and Ge, we assume a Z^2 scaling. With this assumption the observed rate in DAMA remains higher than the upper limit in CDMS. Under the conservative assumption that the modulation amplitude is 6% of the total rate we obtain upper limits on the modulation amplitude a factor of $\sim$2 lower than observed by DAMA, constraining some possible interpretations of this modulation.

　　　　　　　　PACS numbers: 29.40.−n, 29.40.Wk, 85.25.Oj, 95.30.Cq

Astrophysical observations strongly suggest that non-luminous, nonbaryonic matter constitutes most of the matter in the Universe. This dark matter should be distributed in dark halos of galaxies such as the Milky Way, enabling the direct detection of the dark matter particles via their interaction in terrestrial detectors. The movement of the Earth around the Sun would provide an annual modulation of the counting rate, caused by the change in the relative velocity of the dark matter particles and the earthbound

target [1]. The DAMA collaboration claims the observation of such a modulation in two different NaI(Tl) scintillation detector arrays, the original DAMA/NaI setup [2] and the upgraded DAMA/LIBRA experiment [3]. The observed signal is in the 2–6 keV electron-equivalent energy range with a periodicity of 0.998 ± 0.003 years and a phase of 144 ± 8 days. The DAMA collaboration claims that no known systematic detector effect could explain the modulation signal. The modulation phase is consistent with the

expected signature of galactic dark matter inter-acting in a terrestrial detector. However, the original inter-pretation of the DAMA result as a signal from weakly interacting massive particles (WIMPs) that would interact via nuclear recoils [2] is inconsistent with other experi-mental results [4–10]. Also leptophilic dark matter scenar-ios, in which dark matter has tree-level interactions only with leptons, are disfavored as an explanation of the annual modulation signature observed by DAMA, since in such scenarios loop-induced hadron interactions dominate [13]. Note, that the DAMA detectors do not discriminate be-tween electron recoils and nuclear recoils.

A signal from an electromagnetic dark matter interac-tion should be detectable in the cryogenic dark matter search (CDMS) experiment, but would be rejected in our standard search for nuclear recoils [4]. The possibility of an electron-recoil signal from axionlike dark matter parti-cles has recently been investigated [14–16]. In this paper, we present a general analysis of our low-energy electron-recoil spectrum, provide details on the observed counting rate in this energy range, and comment on the implications of these results for possible interpretations of the energy spectrum and the modulation signal observed by DAMA.

The CDMS collaboration operates a total of 19 Ge and 11 Si crystal detectors, each having a mass of ∼250 g and ∼100 g, respectively, at a temperature of ∼40 mK in the Soudan Underground Laboratory [17,18]. The ionization and phonon energy of every event is read out simulta-neously. The recoil energy is reconstructed from them. The ratio of ionization to recoil energy, the ionization yield, discriminates nuclear- from electron-recoil events.

In this analysis we consider data with a total exposure of 443.2 kg-days before cuts, which has been acquired in two run periods between October 2006 and July 2007 (desig-nated as R123 and R124) and is the same data set used for an axion search analysis [16]. Three of the 19 Ge detectors were excluded because of readout failures and another one due to reduced trigger performance at low energies. From the remaining 15 Ge detectors one suffered from reduced trigger performance in R123 and two from incomplete neutralization in R124 which have also been left out of the analysis. The silicon detectors were not considered. We required that an event had to pass several cuts. The events needed to have an ionization energy at least 3σ above the mean noise and be recorded in only one detector. All 30 detectors were used to select these single-scatter events. Moreover, we demanded that there was no signal in the scintillator veto shield surrounding the detectors. The length of the veto coincidence window was set to 50 μs. In order to explore the low-energy electron-recoil spectrum we selected events inside the 2σ electron-recoil band in ionization yield [4]. The fiducial volume was measured using nuclear-recoil events from calibrations with a ^{252}Cf source because of the uniform distribution of neutrons throughout the detector. We excluded all data sets taken

within 3 days after a neutron calibration to avoid high gamma rates due to activation of the predominantly copper detector supporting structure. The remnant rate of ^{64}Cu contributes less than 2% to the mean counting rate at low energies, and decreases with a half life of 12.7 h.

The summed background spectrum of all considered detectors, taking into account the detection efficiency [16], is shown in Fig. 1. For reference, the corresponding counting rates are also given in Table I. In this analysis we consider the electron-equivalent energy range between 2 and 8.5 keV based on the ionization signal, in which the mean background rate is ∼1.5 events/kg/day/keV. Figure 1 also illustrates a simple fit to the observed electron-recoil spectrum. The fit incorporates known spec-tral lines at 10.36 keV and 8.98 keV, both outside of our analysis window. The former is caused by X-rays and Auger-electrons from the decay of ^{71}Ge, a product of neutron capture on ^{70}Ge during neutron calibrations. The latter originates in the decay of remnant ^{65}Zn from cosmo-genic activation of the detectors. We also fit for a spectral line corresponding to an excess of events observed near 6.5 keV, which is likely caused by the deexcitation of ^{55}Mn; this feature is discussed further below. Each peak is fit by a Gaussian distribution function with width fixed at CDMS's measured energy resolution [16]. The detector-averaged rms energy resolution $\sigma(E)$ below 10 keV is given by:

$$\sigma(E) = \sqrt{(0.293)^2 + (0.056)^2 E} \text{ [keV]}, \qquad (1)$$

where E is the measured energy in keV.

^{55}Mn can be produced from electron capture of remnant ^{55}Fe from cosmogenic activation. The deexcitation of
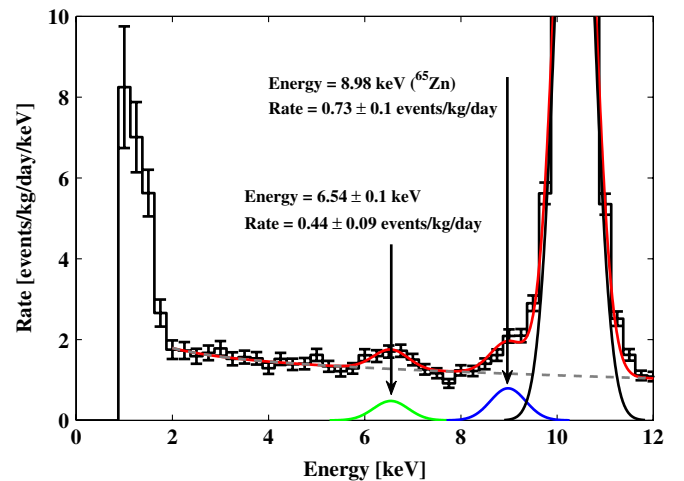

FIG. 1 (color online). Fit (red line) to the efficiency corrected low-energy spectrum consisting of a background model (gray/dashed) and three Gaussian distribution functions describing the 10.36 keV line from ^{71}Ge (black), the 8.98 keV line from ^{65}Zn (blue) and a line at the energy of ^{55}Mn (green, see text). The total counting rate of the latter two lines is given in the figure.

TABLE I.   Rate [events/kg/day/keV] in the 2–8.5 keV energy range.

Energy	Rate	Energy	Rate	Energy	Rate
2.0	1.93 ± 0.24	4.25	1.52 ± 0.15	6.5	1.70 ± 0.15
2.25	1.96 ± 0.22	4.5	1.50 ± 0.15	6.75	1.84 ± 0.16
2.5	1.63 ± 0.19	4.75	1.55 ± 0.15	7.0	1.43 ± 0.14
2.75	1.73 ± 0.18	5.0	1.52 ± 0.15	7.25	1.47 ± 0.14
3.0	2.04 ± 0.19	5.25	1.43 ± 0.14	7.5	1.26 ± 0.13
3.25	1.40 ± 0.15	5.5	1.32 ± 0.13	7.75	1.03 ± 0.12
3.5	1.70 ± 0.17	5.75	1.19 ± 0.13	8.0	1.29 ± 0.13
3.75	1.65 ± 0.16	6.0	1.75 ± 0.15	8.25	1.31 ± 0.13
4.0	1.41 ± 0.15	6.25	1.73 ± 0.15	8.5	1.40 ± 0.13

[55]Mn results in a spectral line at 6.54 keV, matching exactly the energy of the corresponding peak in our spectrum. While at the surface the detectors were exposed to fast neutrons from cosmic-ray showers. Gamma-rays from isotopes produced in Ge by these fast cosmic-ray neutrons have been observed in the CoGeNT experiment, which uses a p-type contact germanium detector providing an excellent energy resolution [15]. The most dominant lines in their spectrum are from [65]Zn with an energy of 8.98 keV and [68,71]Ge with an energy of 10.36 keV, which are both also visible in our spectrum. Calculations of the production rate of cosmogenic isotopes show that [55]Fe is produced in Ge [19]. The 2.73 y half-life of [55]Fe allows a remaining activity of this isotope in the detectors. Since the activation stopped when the detectors were moved underground, the time evolution of this counting rate would enable us to determine if it is caused by [55]Fe isotopes. However, the uncertainties in the production rate and in the time the detectors spent at the surface are too large to permit a reliable constraint on the total rate expected from the deexcitation of [55]Mn.

We carried out a profile likelihood analysis in order to search for a peaked excess of event rate above background [20]. The event rate per unit measured energy (E) and per detector (d) including background was written as:

$$R(E, d) = B(E, d) + A(E, d). \qquad (2)$$

The background $B(E, d)$ is assumed to be of the form

$$B(E, d) = \varepsilon(E, d) \cdot \left[C(d) + D(d)E + \frac{H(d)}{E} \right]$$
$$+ \eta \cdot \varepsilon(E, d) \cdot \frac{\lambda_{6.54}}{\sqrt{2\pi}\sigma_{6.54}(d)}$$
$$\times e^{-((E-6.54)/(\sqrt{2}\sigma_{6.54}(d)))^2}, \qquad (3)$$

where $C(d)$, $D(d)$ and $H(d)$ are free parameters determined by the fit routine, and $\varepsilon(E, d)$ is the energy-dependent detection efficiency. The Gaussian represents a contribution from [55]Fe decays at an energy of 6.54 keV. $A(E, d)$ represents a peaked signal contribution at a given energy E_0. Thus, we used a Gaussian distribution function to

account for the detectors' energy resolution, multiplied with the detection efficiency:

$$A(E, d) = \varepsilon(E, d) \cdot \frac{\lambda_0}{\sqrt{2\pi}\sigma_0(d)} e^{-((E-E_0)/(\sqrt{2}\sigma_0(d)))^2}. \qquad (4)$$

Since we have no constraint on the [55]Fe contribution to the spectrum we do not subtract a possible background contribution. The reason for introducing the additional factor η in (3) is that, while scanning over the recoil energy and approaching the 6.54 keV background peak, the fit function actually consists of a sum of two Gaussians at the same energy. Thus, it serves as a weight suppressing the importance of the [55]Fe rate in the background model $B(E, d)$. $\lambda_{6.54}$ was fixed at the value found by a maximum likelihood fit with $A(E, d) = 0$ and $\eta = 1$. We varied η in steps of 0.1 between 0 and 1 and took the most conservative of these limits for each E_0.

The fit was performed by a maximization of the unbinned log-likelihood function

$$\log(\mathcal{L}) = -R_T + \sum_{i,j} \log R(E_i, d_j), \qquad (5)$$

where the sum goes over events (i) and detectors (j), with respect to λ_0 and the background parameters. R_T denotes the total sum of the event rate (R) over energy and all detectors. We find no statistically significant excess of the event rate above background. We set a Bayesian 90% confidence level (CL) upper limit on the total counting rate λ_0 by integrating the profile likelihood function in the physically allowed region ($\lambda_0 > 0$).

The annual modulation signature observed by DAMA [3] may be interpreted as the conversion of a dark matter particle into electromagnetic energy in the detector. In this case it should be possible to observe the corresponding signal in the electron-recoil spectrum of CDMS. The upper limits on an excess rate presented in this paper should thus help to identify or constrain possible models which can explain the annual modulation signature observed by DAMA. The total counting rate above background observed by DAMA/LIBRA in the claimed signal region has been obtained from a fit to their spectrum consisting of a Gaussian and a background model shown in Fig. 2 giving a rate above background of 0.698 ± 0.051 events/kg/day. A direct comparison between the 90% CL upper limits from this analysis (black/solid) and the rate observed by DAMA (black data point with 2σ error bars in the figure) is shown in Fig. 3. At the energy of the DAMA peak (3.15 keV) the observed rate is inconsistent with the upper limit on the rate in CDMS of 0.246 events/kg/day. Assuming the peak in Fig. 2 is entirely signal, there is an almost 9 standard deviation discrepancy between the DAMA and CDMS results, but very likely background reduces that difference. The peak of Fig. 2 may contain a contribution from the decay of [40]K and the subsequent deexcitation of [40]Ar resulting in a
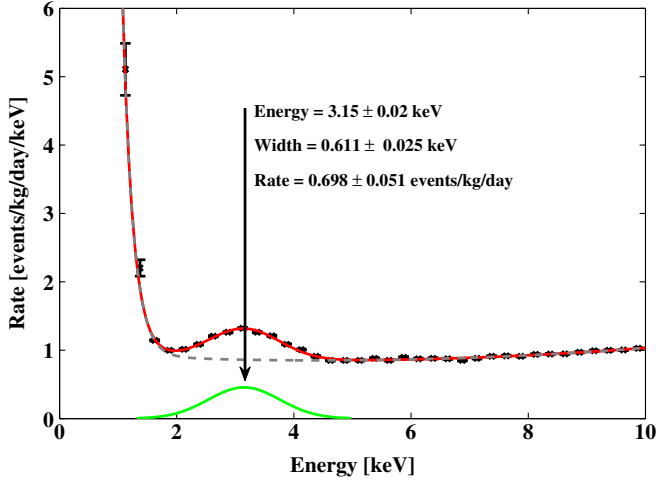
FIG. 2 (color online). Fit (red) to the published DAMA/ LIBRA low-energy spectrum [3], consisting of a background model (gray/dashed) and a Gaussian distribution function (green). The parameters of the Gaussian are given in the figure.

spectral line at 3.2 keV, but no information is supplied on the actual rate of such a background [21]. Thus, no subtraction, which would reduce the difference between the upper limit from CDMS and the excess rate in DAMA, is performed.
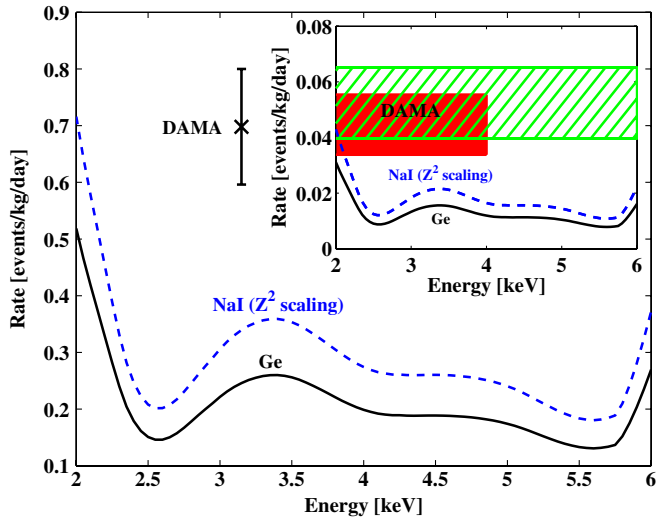

FIG. 3 (color online). 90% CL upper limit on the total counting rate in Ge from this analysis (black/solid). The corresponding upper limit on the total counting rate in NaI under the assumption of a Z^2 scaling of the conversion cross section (see text) is also shown (blue/dashed). The black data point with 2σ error bars gives the total counting rate of the 3.15 keV peak of DAMA/LIBRA derived from a fit to their spectrum (see Fig. 2). The insert compares the upper limit on the modulation amplitude assumed to be 6% of the unscaled upper limit (black/solid) and the Z^2 scaled upper limit in NaI (blue/dashed) with the 2σ regions of the annual modulation amplitude observed by DAMA (NaI + LIBRA) in the 2–4 keV (red/filled) and 2–6 keV (green/hatched) energy range.

Currently there are two studies on the ^{40}K background contribution to the total rate in the DAMA spectrum. The DAMA collaboration showed that the ^{40}K rate is a dominant component [22]. This leads to high ratios of the modulated to unmodulated signal counting rate which are inconsistent with the expected ratio in a standard halo model. On the other hand, an independent Monte Carlo based analysis of the DAMA spectrum claims that the ^{40}K contamination of the crystals [21] are too small to account for the excess rate observed in the unmodulated spectrum [23]. In order to account for this background contribution these discrepancies need to be resolved.

The event rates in the CDMS and DAMA detection media may differ depending on the coupling of the dark matter particle. Thus, the upper limits in Ge have to be scaled to the expected rate in NaI in order to perform a comparison in a particular model. For an electromagnetic conversion of a dark matter particle, the particle velocity is essentially irrelevant (in contrast to the calculation for nuclear recoils, where the energy threshold provides a minimum velocity for the phase space integral). Thus, the annual modulation signature is only caused by a change in the particle flux over the course of the year. The total counting rates per unit mass of such a conversion in the case of a Ge and a NaI target are related by the following condition:

$$\frac{R_{\mathrm{NaI}}}{R_{\mathrm{Ge}}} = \frac{A_{\mathrm{Ge}}}{A_{\mathrm{I}} + A_{\mathrm{Na}}} \cdot \frac{\sigma_{\mathrm{I}} + \sigma_{\mathrm{Na}}}{\sigma_{\mathrm{Ge}}}, \qquad (6)$$

where A_i is the atomic mass of the nuclei, and σ_i is the total cross section per atom of the interaction. The detection efficiencies in both materials should be very close to 100% at these low energies; thus, effects of a material and detector geometry dependent detection efficiency are neglected in the following.

The total cross section will depend on the coupling of the dark matter particle to the detection media. For an electromagnetic conversion a Z^2 (where Z is the atomic number) scaling of the cross section is natural and is thus considered in the comparison of the rate limits in Ge from this analysis with the rate observed by DAMA. Another scaling can be trivially considered. This is a more general comparison than the one considered in our axion search paper [16]. The scaled rate limits in NaI at a 90% CL are given in Fig. 3 (blue/dashed line). The total counting rate observed by DAMA/LIBRA remains greater than the upper limit at 3.15 keV.

Under standard halo assumptions a conservative upper limit on the modulation amplitude is ±6% if the modulation is caused by a change in the particle flux only [24]. Note, that if the conversion cross section is inversely proportional to the dark matter particle velocity (as inelastic cross sections tend to be [25]) the annual modulation amplitude is highly suppressed. The insert in Fig. 3 compares the unscaled upper limit (black/solid) and the Z^2 scaled upper limit in NaI (blue/dashed) on the modulation

amplitude with the 2σ regions of the annual modulation amplitude observed by DAMA (NaI + LIBRA) in the 2–4 keV (red/filled) and 2–6 keV (green/hatched) energy range [3]. The upper limits on the modulation amplitudes are a factor of ~ 2 lower than observed by DAMA.

In this paper we reported on our analysis of the low-energy electron-recoil spectrum of the CDMS experiment, providing the observed rate in the 2–8.5 keV range and the identification of possible background sources. The analysis sets upper limits on the total counting rate of a peaked signal above the background model, in the energy range of 2–8.5 keV. Considering the conversion of a dark matter particle into electromagnetic energy, the 90% CL upper limit on the total counting rate from CDMS at 3.15 keV is below the excess rate observed by DAMA in a direct comparison and under the assumption of a Z^2 scaling of the cross section. This comparison neglects a possible background contribution from ^{40}K in the DAMA data. To include this background in a quantitative analysis would require the knowledge of the actual rate, which is not available. We note that the actual scaling between Ge and NaI has to be provided by a specific model, but stress that an analysis of the low-energy electron-recoil spectrum of CDMS helps to identify or constrain possible models which can explain the annual modulation signature observed by DAMA. In the conservative case of a 6% modulation amplitude our recent data provides 90% CL upper limits on the modulation amplitude that are a factor of ~ 2 less than observed by DAMA.

[1] A. K. Drukier, K. Freese, and D. N. Spergel, Phys. Rev. D **33**, 3495 (1986).
[2] R. Bernabei *et al.*, Phys. Lett. B **480**, 23 (2000).
[3] R. Bernabei *et al.*, Eur. Phys. J. C **56**, 333 (2008).
[4] Z. Ahmed *et al.*, Phys. Rev. Lett. **102**, 011301 (2009).
[5] J. Angle *et al.*, Phys. Rev. Lett. **100**, 021303 (2008).
[6] J. Angle *et al.*, Phys. Rev. Lett. **101**, 091301 (2008).
[7] E. Behnke *et al.*, Science **319**, 933 (2008).
[8] H. S. Lee *et al.*, Phys. Rev. Lett. **99**, 091301 (2007).
[9] V. N. Lebedenko *et al.*, Phys. Rev. D **80**, 052010 (2009).
[10] There are scenarios, such as micro-channeling effects of ions in crystals, which still leave some allowed parameter space at low WIMP masses (~ 10 GeV range) [11,12].
[11] E. M. Drobyshevski, Mod. Phys. Lett. A **23**, 3077 (2008).
[12] R. Bernabei *et al.*, Eur. Phys. J. C **53**, 205 (2008).
[13] J. Kopp *et al.*, Phys. Rev. D **80**, 083502 (2009).
[14] R. Bernabei *et al.*, Int. J. Mod. Phys. A **21**, 1445 (2006).
[15] C. E. Aalseth *et al.*, Phys. Rev. Lett. **101**, 251301 (2008).
[16] Z. Ahmed *et al.*, Phys. Rev. Lett. **103**, 141802 (2009).
[17] K. D. Irwin *et al.*, Rev. Sci. Instrum. **66**, 5322 (1995); T. Saab *et al.*, AIP Conf. Proc. **605**, 497 (2002).
[18] D. S. Akerib *et al.*, Phys. Rev. D **72**, 052009 (2005).
[19] D.-M. Mei, Z.-B. Yin, and S. R. Elliot, Astropart. Phys. **31**, 417 (2009).
[20] F. James, *Statistical Methods in Experimental Physics* (World Scientific Publishing Co. Pte. Ltd., Singapore, 2005), 2nd ed..
[21] R. Bernabei *et al.*, Nucl. Instrum. Methods Phys. Res., Sect. A **592**, 297 (2008).
[22] R. Bernabei *et al.*, arXiv:0912.4200v1.
[23] V. A. Kudryavtsev, M. Robinson, and N. J. C. Spooner, arXiv:0912.2983v1.
[24] J. D. Lewin and P. F. Smith, Astropart. Phys. **6**, 87 (1996).
[25] M. Pospelov, A. Ritz, and M. Voloshin, Phys. Rev. D **78**, 115012 (2008).